

# Flagella-like beating of a single microtubule

Andrej Vilfan,<sup>1,2,\*</sup> Smrithika Subramani,<sup>1,\*</sup> Eberhard Bodenschatz,<sup>1,3,4</sup> Ramin Golestanian,<sup>1,5</sup> and Isabella Guido<sup>1,†</sup>

<sup>1</sup>Max Planck Institute for Dynamics and Self-Organization (MPIDS), 37077 Göttingen, Germany

<sup>2</sup>Jožef Stefan Institute, 1000 Ljubljana, Slovenia

<sup>3</sup>Institute for Dynamics of Complex Systems, Georg-August-University Göttingen, 37073 Göttingen, Germany

<sup>4</sup>Laboratory of Atomic and Solid-State Physics, Cornell University, Ithaca, NY 14853, United States

<sup>5</sup>Rudolf Peierls Centre for Theoretical Physics, University of Oxford, Oxford OX1 3PU, United Kingdom

Kinesin motors can induce a buckling instability in a microtubule with a fixed minus end. Here we show that by modifying the surface with a protein-repellent functionalization and using clusters of kinesin motors, the microtubule can exhibit persistent oscillatory motion, resembling the beating of sperm flagella. The observed period is of the order of 1 min. From the experimental images we theoretically determine a distribution of motor forces that explains the observed shapes using a maximum likelihood approach. A good agreement is achieved with a small number of motor clusters acting simultaneously on a microtubule. The tangential forces exerted by a cluster are mostly in the range 0 – 8 pN towards the microtubule minus end, indicating the action of 1 or 2 kinesin motors. The lateral forces are distributed symmetrically and mainly below 10 pN, while the lateral velocity has a strong peak around zero. Unlike well-known models for flapping filaments, kinesins are found to have a strong “pinning” effect on the beating filaments. Our results suggest new strategies to utilize molecular motors in dynamic roles that depend sensitively on the stress built-up in the system.

## INTRODUCTION

The propulsion of motile cells such as sperms rely on undulating bending of flagella, appendages of the cellular body able to perform periodic oscillations. This beating is driven by the interaction between microtubules and motor proteins and the mechanism that regulate these interactions, as well as, how they can orchestrate complex vital processes are not well understood yet. The functional reactions of living systems operating out of equilibrium are the result of component rearrangements due to the intrinsic stochasticity in the system itself. Building a synthetic molecular system in which components continuously rearrange and reorganize in the presence of energy sources would enable a deep understanding of these molecular interactions.

Here we present experimental and theoretical results on a minimal system made of a single microtubule with a fixed end and a small number of kinesin-1 motor proteins (kinesin hereafter) that in the presence of ATP perform a continuous motion resembling the beating of sperm flagella.

In the past decades these components were used in *in vitro* gliding assay [1, 2] where the motor proteins were attached on the surface of a glass coverslip at high density. Directed sliding motion of filaments was enabled when they came into contact with the surface bound motors. Previous studies showed microtubule buckling in a low density gliding assay due to a single kinesin motor [3], waving and rotating motion of biofilaments in gliding assay [4, 5] as well as spiral formation of microtubules caused by pinning at the leading end [4] and by the interactions with neighboring microtubules [6].

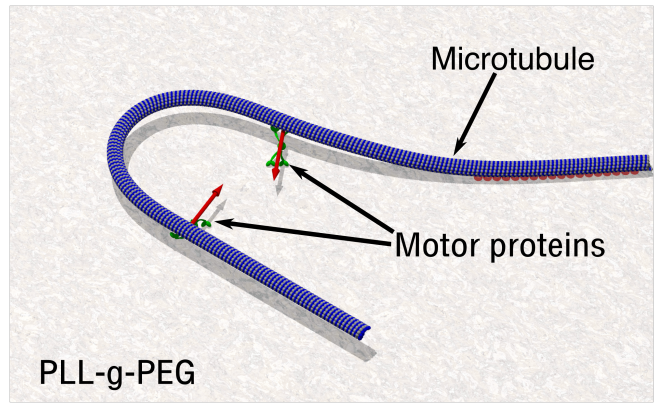


FIG. 1. Schematic representation of the minimal system. A single filament clamped at one end beating and buckling under the action of motor proteins interacting with PLL-g-PEG functionalized surface.

In this study we quantitatively analyze the buckling instabilities of single microtubules clamped at one end and subjected to the forces exerted by motor proteins. We found that by using a specific surface treatment for the substrate and organizing the motors in randomly distributed clusters we obtain filaments that perform continuous beating.

We can describe the system as follows (Fig. 1): (i) the kinesin motors in the cluster simultaneously bind either to the microtubules or unspecifically to the surface; (ii) the motors exert forces on the microtubule which are directed along the tangential direction. Above a threshold the straight configuration of the filament becomes unstable inducing the buckling of the filament; (iii) the force that bends the filament has a longitudinal component

as well as a perpendicular component that allows the microtubule to snap back to its straight configuration. This can be explained by either the filament detaching from the motors or by the motors breaking the bond with the protein-repellent surface and being pulled away while remaining attached to the filament. Both lead to a subsequent buckling when the filament reaches the new position. The behaviour of the system is self-organized by the elasticity of the filament, the active forces exerted by motor proteins and by using attachment and detachment between the building blocks of this minimal system.

## RESULTS AND DISCUSSION

*Experimental results* Here, we report the quantitative analysis of buckling instabilities of clamped microtubules caused by compressive forces exerted by kinesin motors. Diluted polymerized microtubules of approx. 8  $\mu\text{m}$  length were decorated with motor protein clusters by mixing them with biotinylated kinesin clustered by using streptavidin. The surface was functionalized by using PLL-g-PEG (see Materials and Methods section). This nonionic polymer has been proven to limit biological interactions [7] and in this set-up it prevents irreversible protein adsorption on the surface. A sample of the microtubules-kinesins mixture was poured on the PLL-g-PEG modified cover slip and the experimental chamber was sealed in order to avoid any artefacts caused by fluid streaming. In our experiments the chosen functionalization of the glass surface almost entirely avoids the microtubules adsorption. However, we could occasionally observe microtubules with one tip clamped (typically 2  $\mu\text{m}$ ) to the surface (1-2 samples in each experiment) likely due to electrostatic interaction with the polylysine backbone of the PLL-g-PEG functionalization. The anchor point had no rotational or translational degree of freedom. The free part of the microtubule was observed to perform oscillatory motion as shown in Fig. 2. This motion is attributed to the kinesin motors which could bind with their heads attached to the microtubule and unspecifically bound to the surface simultaneously, due to their organization in clusters. When the kinesin-clusters were bound in this manner the motors transiently pushed the filament forward resulting in cyclic conformational changes for time intervals up to 5 minutes. The oscillations of the microtubule can be divided into cycles, defined as the time that the filament needs to move from one portion of the space to the adjacent one and to come back (2-A). The filament tracking of one cycle is exemplarily shown in figure 2-C where the four subsequent positions are overlaid and labeled in order to show the beating behaviour of the microtubule.

The ability to beat and buckle persistently depends on (i) an optimal concentration of motor clusters and (ii) an interacting surface with a drastically reduced pro-

tein adsorption. Control experiments carried out without a PLL-g-PEG surface functionalization showed no buckling filaments, proving that the unspecific binding of both motor proteins and microtubules does not allow any filament to move freely.

The motor concentration needed to buckle the filament can be estimated from the following simple argument. A filament of length  $L$  is attached to motor clusters with an average spacing  $\lambda$ , which we treat as pinning points. If we assume that the filament is torque-free at the motor positions (which is a simplification), the force needed to buckle the segment is

$$F_B = \frac{\pi^2 EI}{\lambda^2}. \quad (1)$$

The compressive force, exerted by the ensemble of motors, is highest in the segment next to the clamped end, and corresponds to  $F_M L/\lambda$ , where  $F_M$  is the stall force of a motor cluster. Both become equal at a critical length

$$L_C = \frac{\pi^2 EI}{F_M \lambda}, \quad (2)$$

which is inversely proportional to the motor spacing or proportional to their density. With the values  $F_M = 8 \text{ pN}$ ,  $EI = 0.4 \times 10^{-23} \text{ Nm}^2$  and  $\lambda = 1 \mu\text{m}$ , we obtain  $L_C = 5 \mu\text{m}$ . A filament of this length will generally buckle if the number of motors acting on it is in the range 1-5.

We verified the importance of the motor protein concentration by repeating the experiments with a different motors concentration. The experiments showed a reduced capacity to buckle continuously. By using a 100-fold higher concentration not continuous oscillations were observed. The buckling events were less frequent and limited in time compared to the analysed case (movie S2). By reducing 2-fold the concentration again the buckling events were less frequent and limited in time as the sliding of filaments was followed by the filaments leaving the focal plane due to the missing grasp (movie S3).

We analyze the movement pattern of our filaments. Their beating was observed to be quasi 2D and this allowed us to track the filament shape. We characterized the tracked filament shape by a tangent angle  $\psi(s,t)$ , which describes the angle between the straight line representing the initial position of the filament and the local tangent of the arclength  $s$  along the filament at the time  $t$  with  $0 \leq s \leq L$  and  $L$  the length of the free moving filament portion (Fig. 2-D). We tracked the shape changes for  $n$  frames with  $n$  up to 300. We obtained a matrix  $\psi(s,n)$  that represents the kymograph of the filament movement (Fig. 2-D). We can observe a pattern indicating a wavy motion propagating from one end of the filament along its entire length and reflecting the periodicity of the filament beating, i.e. the four cycles which its movement can be divided into, as defined above and

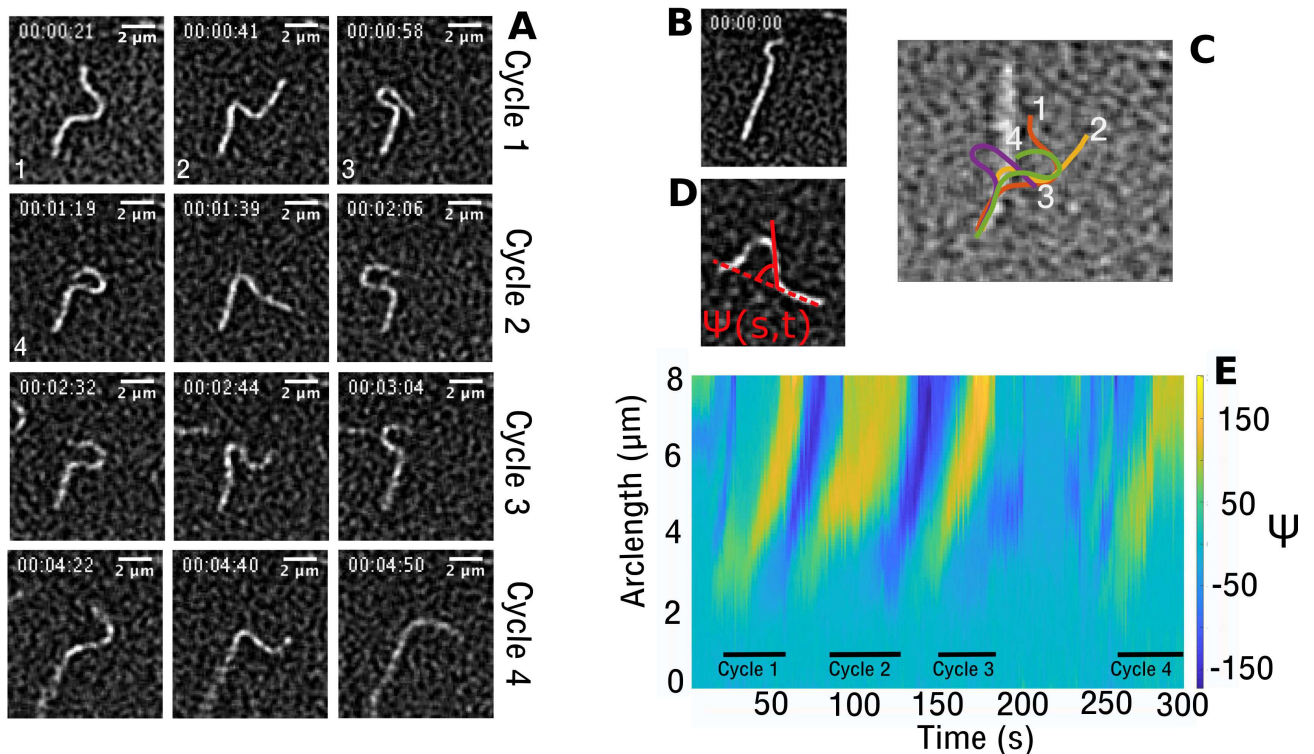


FIG. 2. A. Oscillation cycles of a single filament clamped on the surface over time starting at  $t=0$  from the configuration shown in B. B. Starting position of clamped filament. C. Filament tracking shows the time evolution of the emergent oscillations. For visualization reason only the tracking of first cycle is shown. The numbers indicate the chronology of the oscillation as well as correspond to the filament positions shown in A (see numbers on the bottom left of the micrographs). D. Tangent angle  $\psi(s,t)$  as a function of arclength  $s$  along the flagellum. E. Kymograph of the tangent angle over time along the filament. The oscillation and its duration corresponding to each cycle is pointed out in the figure.

depicted in Fig. 2-A. Thus, the beating profile shown in Fig. 2-E, is similar to the beating of eukaryotic flagella.

The analogy between filaments subject to tangential compressive forces and beating flagella has already been pointed out in several theoretical studies. The basic problem consists of a semiflexible polymer with one clamped end, subject to local drag and an active tangential force. Sekimoto et al. [5] showed the existence of a dynamical instability, above which the filament undergoes flapping motion, whereas Bourdieu et al. [4] briefly presented a waving motion in actin and microtubules. A related problem with a single follower force at the free filament tip was solved in Ref. [8]. If the filament is free to move in 3 dimensions, there is an additional spinning state [9]. If the clamped end is replaced by a cargo, resembling a sperm head, the numerically obtained solutions show rotation or sperm-like beating [10]. Despite the similarities, there are also essential differences between our system and these models. The small number of motors involved makes the dynamics less deterministic, while the ability of kinesins to sustain off-axis loads largely reduces the lateral motion of the filament, except during periods of fast relaxation, presumably caused by

the detachment of motors from the distal region.

We have the conjecture that the continuous buckling dynamics might be also due to the reversible attachment of the motors to the surface, which was tailored to allow a binding that is sufficient stable for activating the 'walk' on the microtubule but so weak to dissociate under mechanical stimulus. In this way the system self-organized by using the force of motor proteins that continuously rearranged by breaking and reforming bonds to the surface. The weak bond to the surface was tested by applying a fluid flow at shear rate estimated as  $4 \times 10^4 \text{ s}^{-1}$  that was able to wash out the motors unspecifically bound to the surface. Other studies show that surface modifications are able to create reversible motors binding responsible for self-organization of microtubules dynamics due to continuous rearrangement of motors distribution [11]. We believe that the force exerted by the motors in one portion of the filament inducing its buckling reached a threshold above which it was able to pull away the other motors from the surface. As soon as the microtubule was not under the constrain of the motors totally or partially relaxed to the straight position due to its elastic properties transporting the motors in another position. After

this rapid position change the reattachment of the motors occurred again and a subsequent new sliding of the filament.

We used a maximum likelihood method to reconstruct a distribution of motor forces that gives the observed filament shape. Examples of filaments with corresponding forces are shown in Fig. 3. The tangential components of the forces (Fig. 3-B) shows a strong accumulation in the range between  $-8$  pN and  $0$  pN (a negative sign denotes forces pushing the filament towards the clamped end, which is the MT minus end), consistent with the forces produced by single kinesin motors. Larger values, up to  $-20$  pN, could result from the action of multiple motors, either within a cluster, or sufficiently close together that they become unresolvable. Normal forces are mostly in the range  $-10$  to  $10$  pN, also consistent with 1-2 kinesins. The tangential velocity of the filament shows a highly skewed distribution, mainly in the range  $-400$  nm/s to  $0$  nm/s (negative sign shows the filament moving towards the clamped end, consistent with the action of kinesins). However, both velocities sometimes exceed  $2$   $\mu$ m/s, namely as the free filament end snaps to a relaxed position.

In conclusion, we report an example of autonomous molecular system that dynamically self-organizes through its elasticity and the interaction with the environment represented by the active forces exerted by motor proteins resembling the beating of a flagellum. Assembling such minimal systems that can mimic the behaviour of much more complex biological structure might help to unveil the basic mechanism underlying the beating of real cilia and flagella.

## MATERIALS AND METHODS

**Non-Adsorbing Surface Coatings and experimental chamber assembly.** Glass coverslips ( $64 \times 22$  mm<sup>2</sup>, VWR) were cleaned by washing with 100% ethanol and rinsing in deionized water. They were further sonicated in acetone for 30 min and incubated in ethanol for 10 min at room temperature. This was followed by incubation in a 2% Hellmanex III solution (Hellma Analytics) for 2h, extensive washing in deionized water and drying with a filtered airflow. The cleaned coverslips are immediately activated in oxygen plasma (FEMTO, Diener Electronics, Germany) for 30 s at 0.5 mbar and subsequently incubated in 0.1 mg/mL Poly(L-lysine)-graft-poly(ethylene glycol) (PLL-g-PEG) (SuSoS AG, Switzerland) in 10 mM HEPES, pH = 7.4, at room temperature for 1 h on parafilm (Pechiney, U.S.A.). Finally, the coverslips were lifted off slowly and the remaining PLL-g-PEG solution was removed for a complete surface dewetting. The experimental chamber was obtained by cutting a window ( $8$  mm $\times$  $8$  mm) on double-sided tape of thickness 10  $\mu$ m (No. 5601, Nitto Denk Corporation, Japan)

and sandwiched between two functionalized coverslips.

**Kinesin-1 Decorated Microtubules Experiments.** Microtubules were polymerized from 2.7 mg/ml HiLyte<sup>TM</sup> labeled porcine brain tubulin (Cytoskeleton, Inc., U.S.A.) in M2B (80 mM PIPES, adjusted to pH = 6.9 with KOH, 1 mM EGTA, 2 mM MgCl<sub>2</sub>) with 5 mM MgCl<sub>2</sub>, 1 mM GTP, 5% DMSO at 37 °C for 30 min. The microtubules were stabilized and diluted 2000-fold in M2B containing 7  $\mu$ M taxol. The plasmid that codes biotin-labeled kinesin 401 (K401) was a gift from Jeff Gelles (pWC2 - Addgene plasmid # 15960 ; <http://n2t.net/addgene:15960>; RRID\_Addgene\_15960) [12]. Kinesin 401 was purified as previously published [13, 14] and the kinesin-streptavidin complexes were prepared by mixing 0.2 mg/ml kinesin 401, 0.9 mM dithiothreitol (DTT), 0.1 mg/ml streptavidin (Invitrogen, S-888) dissolved in M2B and incubated on ice for 15 min. 4  $\mu$ l of this mixture was mixed with 0.5 mg/ml glucose, 0.65 mM DTT, 0.2 mg/ml glucose oxidase (Sigma G2133), 0.05 mg/ml catalase (Sigma C40), 1 mM ATP, 1.7  $\mu$ l pyruvate kinase/lactic dehydrogenase (PK/LDH, Sigma, P-0294), 32 mM phosphoenol pyruvate (PEP, VWR AAB20358-06), 2.4 mM Trolox (Sigma 238813) to form an active clusters solution. The microtubules and active clusters solution in different concentrations were mixed 15 min before use according to the intended experiments. 2  $\mu$ l of this mixture were pipetted onto the PLL-PEG functionalized glass and the experimental chamber was sealed.

**Imaging and Tracking.** Image acquisition was performed using an inverted fluorescence microscope Olympus IX81 (Olympus, Japan) with a 63 $\times$  oil-immersion objective (Olympus, Japan). For excitation, a Lumen 200 metal arc lamp (Prior Scientific Instruments, U.S.A.) was applied. The data was recorded with a Photometrics Cascade II EMCCD camera ( $512 \times 512$  px). The images were acquired every 1 s with an exposure time of 100 ms. The microtubule trajectory was manually tracked by tracing the filament contour using JFilament, an ImageJ plugin for segmentation and tracking [15].

**Reconstruction of Kinesin Forces.** To determine a minimal configuration of forces that can lead to the observed shapes, we maximized the quantity

$$\ell = - \int_{L_0}^L (\Delta(s))^2 ds - \mu \sum_{i=1}^{N_f} \mathbf{f}_i^2 - \nu N_f. \quad (3)$$

Here  $\Delta$  denotes the shortest distance between a point on the experimental and the shape, calculated from the forces. The integral runs over the part of the filament that is free to move, as obtained from an analysis of lateral fluctuations. The second and the third term were introduced to avoid overfitting: they penalize solutions with excessive forces or with too many parameters. For a collection of forces,  $\mathbf{f}_1, \dots, \mathbf{f}_{N_f}$ , located at positions  $s_1, \dots, s_{N_f}$ , the expected filament shape is calculated from

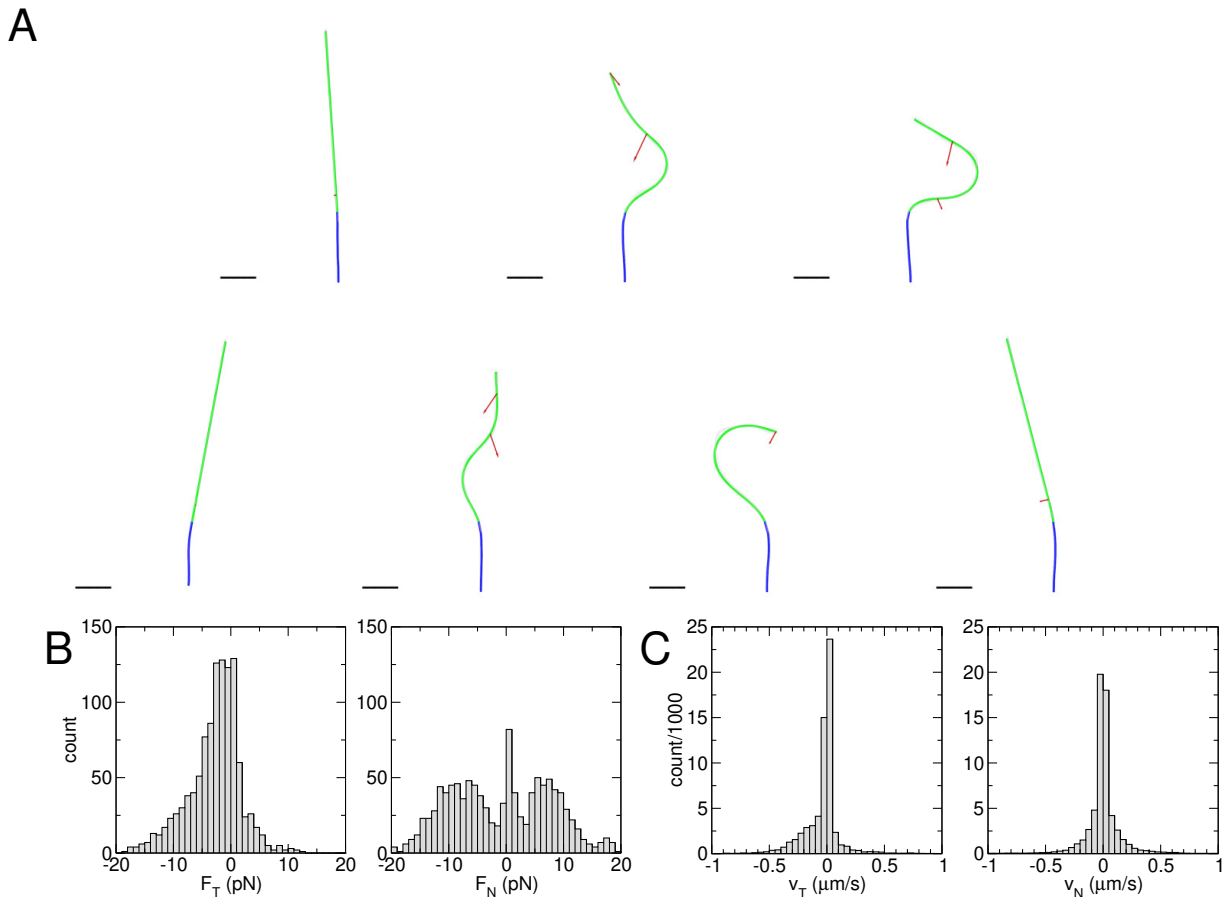


FIG. 3. A. Reconstruction of motor forces (red arrows) from filament shapes (gray: experimental; green: fitted; blue: fixed filament end). Scale bar:  $1 \mu\text{m}$ ,  $10 \text{ pN}$ . B. Distribution of tangential (T) and normal (N) force components. A negative sign ( $F_T < 0$ ) represents a force pushing the microtubule towards the clamped end. C. Tangential and normal velocity components of points on the filament.  $v_T < 0$  indicates the filament moving towards the clamped end. The histograms were obtained from the analysis of three continuously beating microtubules over time intervals ranging from 1:30 to 5 minutes.

the equations

$$\frac{d\mathbf{M}}{ds} = -\mathbf{t} \times \left[ \sum_{i=1}^{N_f} \Theta(s_i - s) \mathbf{f}_i \right] \quad (4)$$

$$\frac{d\mathbf{t}}{ds} = \frac{1}{EI} \mathbf{t} \times \mathbf{M} \quad (5)$$

$$\frac{d\mathbf{x}}{ds} = \mathbf{t} \quad (6)$$

with the boundary condition  $\mathbf{M}(L) = 0$ . We assume a planar filament shape, such that  $\mathbf{f}_i$ ,  $\mathbf{x}$  and  $\mathbf{t}$  lie in the horizontal plane and  $\mathbf{M}$  perpendicular to it. We solve the differential equations (4-6) numerically and evaluate the deviation of the solution from the experimental shape  $\Delta(s)$ . Examples of reconstructed force distributions for one experiment are shown in Fig. 3-A.

The authors thank the MaxSynBio Consortium which is jointly funded by the Federal Ministry of Education and Research of Germany and the Max Planck Society.

## SUPPLEMENTAL MOVIES

- S1: Time-lapse movie of the reconstruction of force distribution acting on the microtubule.
- S2: Time-lapse movie of an experimental assay carried out by using a 100-fold higher motor protein concentration.
- S3: Time-lapse movie of an experimental assay carried out by using a 2-fold lower motor protein concentration.

\* These authors contributed equally

† isabella.guido@ds.mpg.de

- [1] S. J. Kron and J. A. Spudich, Proc. Natl. Acad. Sci. U.S.A. **83**, 6272 (1986).

- [2] J. Howard, A. J. Hudspeth, and R. D. Vale, *Nature* **342**, 154 (1989).
- [3] F. Gittes, E. Meyhöfer, S. Baek, and J. Howard, *Biophys. J.* **70**, 418 (1996).
- [4] L. Bourdieu, T. Duke, M. B. Elowitz, D. A. Winkelmann, S. Leibler, and A. Libchaber, *Phys. Rev. Lett.* **75**, 176 (1995).
- [5] K. Sekimoto, N. Mori, K. Tawada, and Y. Y. Toyoshima, *Phys. Rev. Lett.* **75**, 172 (1995).
- [6] L. Liu, E. Tüzel, and J. L. Ross, *J. Phys.: Condens. Matter* **23**, 374104 (2011).
- [7] G. L. Kenausis, J. Vörös, D. L. Elbert, N. Huang, R. Hofer, L. Ruiz-Taylor, M. Textor, J. A. Hubbell, and N. D. Spencer, *J. Phys. Chem. B* **104**, 3298 (2000).
- [8] G. De Canio, E. Lauga, and R. E. Goldstein, *J. R. Soc. Interface* **14**, 20170491 (2017).
- [9] F. Ling, H. Guo, and E. Kanso, *J. R. Soc. Interface* **15**, 20180594 (2018).
- [10] R. E. Isele-Holder, J. Jäger, G. Saggiorato, J. Elgeti, and G. Gompper, *Soft Matter* **12**, 8495 (2016).
- [11] A. T.-C. Lam, S. Tsitkov, Y. Zhang, and H. Hess, *Nano Lett.* , 1530—1534 (2018).
- [12] R. Subramanian and J. Gelles, *J. Gen. Physiol.* **130**, 445 (2007).
- [13] S. P. Gilbert and K. A. Johnson, *Biochemistry* **32**, 4677 (1993).
- [14] E. Young, E. Berliner, H. Mahtani, B. Perez-Ramirez, and J. Gelles, *J. Biol. Chem.* **270**, 3926—3931 (1995).
- [15] M. B. Smith, H. Li, T. Shen, X. Huang, E. Yusuf, and D. Vavylonis, *Cytoskeleton* **67**, 693 (2010).